



Determination of time of death in forensic science via a 3-D whole body heat transfer model



Catherine Bartgis, Alexander M. LeBrun, Ronghui Ma, Liang Zhu*

Department of Mechanical Engineering, University of Maryland Baltimore County, Baltimore, MD 21250, United States

ARTICLE INFO

Article history:

Received 10 February 2016

Accepted 5 July 2016

Available online 7 July 2016

Keywords:

Postmortem

Time of death

Temperature

Whole body model

Forensic science

ABSTRACT

This study is focused on developing a whole body heat transfer model to accurately simulate temperature decay in a body postmortem. The initial steady state temperature field is simulated first and the calculated weighted average body temperature is used to determine the overall heat transfer coefficient at the skin surface, based on thermal equilibrium before death. The transient temperature field postmortem is then simulated using the same boundary condition and the temperature decay curves at several body locations are generated for a time frame of 24 h. For practical purposes, curve fitting techniques are used to replace the simulations with a proposed exponential formula with an initial time delay. It is shown that the obtained temperature field in the human body agrees very well with that in the literature. The proposed exponential formula provides an excellent fit with an R^2 value larger than 0.998. For the brain and internal organ sites, the initial time delay varies from 1.6 to 2.9 h, when the temperature at the measuring site does not change significantly from its original value. The curve-fitted time constant provides the measurement window after death to be between 8 h and 31 h if the brain site is used, while it increases 60–95% at the internal organ site. The time constant is larger when the body is exposed to colder air, since a person usually wears more clothing when it is cold outside to keep the body warm and comfortable. We conclude that a one-size-fits-all approach would lead to incorrect estimation of time of death and it is crucial to generate a database of cooling curves taking into consideration all the important factors such as body size and shape, environmental conditions, etc., therefore, leading to accurate determination of time of death.

© 2016 Elsevier Ltd. All rights reserved.

1. Background

Determining postmortem interval is vital to the study of forensic science. Knowing the time of a murder can be used to exonerate or incriminate a person of interest. In the past two centuries, multiple approaches have been developed to determine postmortem interval using biochemical markers as well as physical measurements. Decomposition stages or insect colonization have been suggested as an indication of time of death for bodies found after weeks of being dead. However, due to the uncertainty of the determined time varying more than days or weeks, a more accurate method is to rely on physical measurements, including temperatures at various body locations.

In 1868, Dr. Henry Rainy, a Professor at Glasgow, suggested that the cooling rate of a dead body could be used to determine time of death (Crowther and White, 1988). The formula (Eq. (1)) given below, determines the postmortem interval by having the

pathologist measuring the temperature of the rectum and modeling the temperature decay as a linear function:

Hours after death

$$= \frac{\text{Normal temperature } (98.4^{\circ}\text{F}) - \text{Rectal temperature}}{1.5} \quad (1)$$

This equation suggests that the cooling rate of the body is approximately 1.5 °F per hour. Later this equation was modified to become two linear segments, with the cooling rate as 2 °C per hour for the first 12 h and 1.5 °C per hour for the second 12 h. The accuracy of this approach is poor, because the rate at which a body cools can be affected by various parameters. External air temperature, weather, environment, body size and shape, and initial body temperature distribution all play important roles in determining the cooling rate (Guharaj, 1982).

Due to mathematical advancements in the 19th century, one can derive a partial/ordinary differential equation to describe the body temperature decay process after death. It has been shown that the heat loss from a warm body to a cold environment is governed by the Newton's law of cooling, i.e., the heat transfer rate

* Corresponding author.

E-mail address: zliang@umbc.edu (L. Zhu).

from a body is proportional to the temperature difference at the body surface and the air temperature, as well as the heat transfer coefficient h that is related to the thermal resistance between the surface and its environment. For a transient heat transfer process, a simplified model used is called the “lumped capacitance method”. The lumped capacitance method assumes that a solid of uniform temperature is being put into a fluid at a different temperature (Bergman et al., 2011). This uniform temperature in the solid negates any temperature gradients in the solid. Neglecting the temperature variation within the solid results in an ordinary differential equation (ODE) rather than a partial differential equation for governing the temperature drop, therefore, solving for the ODE is straight forward as:

$$\frac{T(t) - T_{air}}{T_i - T_{air}} = \exp(-t/\tau), \quad \text{where } \tau = \frac{\rho c V}{Ah} \quad (2)$$

where t is time, $T(t)$ is the temperature of the solid, varying with time, T_{air} is air temperature, and T_i is the initial temperature. The result using the lumped capacity method suggests that the normalized temperature (the left side of Eq. (2)) can be described by an exponential function with a time constant τ . The time constant, describing how fast the solid responds to the change of its environment, is related to its density ρ , specific heat c , solid volume V , solid surface area A , and the heat transfer coefficient h , described in the Newton's law of cooling.

Eq. (3) given in some websites estimates the postmortem interval based on the Newton's law of cooling:

$$\text{time (h)} = -10 \ln\left(\frac{T - R_t}{98.6^\circ\text{F} - R_t}\right) \quad (3)$$

It is evident that Eq. (3) is almost the same as Eq. (2) except that the time constant is chosen to be 10 h. Eq. (3) allows determination of the time of death with only a single temperature measurement at the rectum or liver site if the air temperature R_t is known. It also assumes that the initial body temperature is 98.6°F or 37°C .

Eq. (3) based on the Newton's law of cooling is an improvement from the linear temperature decays used previously. This equation is not accurate since it proposes a time constant τ as ten hours. As shown in Eq. (2), the time constant can be greatly influenced by many factors, including the size (volume V), the shape (surface area A), body composition (density ρ , and specific heat c), and the heat transfer coefficient h . A more roundly shaped person (large V/A) has a larger time constant, implying that it is more difficult to lose heat than a skinnier person (small V/A). The amount of fat a person carries varies due to the amount of insulation the body has. If a body is more insulated due to a thicker fat layer, the body temperature will decay at a slower rate. Further improvement in extracting time of death takes into consideration the body size, thermal resistance due to clothes, thermal variations of the environment, and the possibility that an exponential function alone is not accurate to describe the temperature decay. One of the more extensive models for determining the post mortem interval is the Hessnge's Nomogram (Payne-James et al., 2011), proposing that the normalized rectum temperature is described by a combination of two exponential functions with different time constants:

$$\frac{T_{rectum} - T_{ambient}}{37.2 - T_{ambient}} = 1.25\exp(Bt) - 0.25\exp(5Bt) \quad (4)$$

where T_{rectum} is the temperature of the rectum in Celsius, $T_{ambient}$ is the temperature of the external environment, t is time in hours, and B is related to the time constant ($B = -1/\tau$) and is proposed to be related to the body mass in kilogram, W :

$$B = -1.2815(W^{-0.625}) + 0.0284 \quad (5)$$

Note that this formula is only valid for a naked body in still air. Estimation of the time of death for other situations such as wearing clothes, being in a moving fluid or in water can also be determined using a correction factor. For example, when the person wears 1–2 thin layers of clothes in still air, the correct factor is 1.1, implying the actual time of death is longer than that estimated by the formula since the clothes slow down the temperature decay. On the other hand, a naked body in a moving air, the actual time of death is shorter (a correction factor of 0.75) because of the easier heat loss due to strong convection. The proposed formula (Eq. (4)) is more accurate than previous methods since it takes into account the weight of the body, the ambient temperature, the speed of moving fluid, and the clothing a person is wearing. However, it does not take into account the initial stagnation of the temperature. Most importantly, this model is also limited to the user's interpretation of the layers of the clothing. The researchers simply describe clothing as either thick or thin. They do not specify the material or the thickness required to be considered as a “thick material”.

The major limitation of all the previous studies is the rudimentary calculation of the time in the above mentioned simple formulas. It is well known that a dead body loses heat passively by radiation, conduction, and convection to its environment. There are many factors that may influence the three mechanisms, including the size and shape of the body, obesity, heavy clothing, air is moving or still, exposure to direct sunlight, to name a few. Another important issue none of the above studies considered is the body location where the temperature is recorded. It will be very practical to measure the body temperature only once. However, as mentioned above, it is difficult to determine with confidence that one or two measurements of temperature at the same site are sufficient to address all the influencing factors. In another word, without a more rigorous theoretical simulation considering all the factors, it is almost impossible to determine the exact time of death, leading to an erroneous estimation.

This study focuses on developing a whole body heat transfer model to simulate rigorously not only the time decay after death, but also the temperature distribution of the body before death. Although some finite element models were proposed, the initial condition is either assumed as a constant and uniform temperature of 37°C or based on an inaccurate temperature distribution estimation (Mall and Eisenmenger, 2004a, 2004b). In addition, the convection/radiation coefficient between the body and the environment is roughly estimated. It is unknown how they determine the values for individual cases in those previous studies.

In this study, we develop a whole body physical model based on actual measurements of a human body and to use energy balance between local blood perfusion rate and surrounding tissue to determine a lumped “overall heat transfer coefficient”, modeling the total thermal resistance of conduction (clothing layers), convection (moving or still air), and radiation (radiation exchange with the surroundings) when the human body is in thermal equilibrium with its surrounding. The obtained initial temperature field is then substituted into the model to simulate the temperature decay processes at various body measurement sites (internal organ, brain, etc.). For practical use, we also preform curve fitting to a proposed temperature decay formula to identify the time constant and the initial time delay in the proposed temperature cooling curve formula. It is expected that the temperature cooling curve formula would be used to accurately determine the time of death based on one or two measurements of the temperatures at specific body sites.

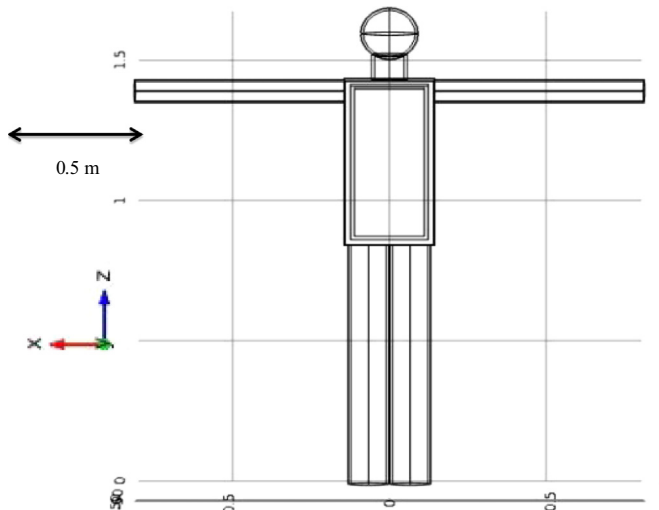


Fig. 1. Developed 3-D whole body heat transfer model in the z-x plane.

2. Methods

2.1. Mathematical formulation of the whole body model

Heat transfer from a human body after death to its environment relies on thermal resistance of conduction, convection, and radiation on the skin surface. The postmortem temperature decay in a human body can also be affected by the initial non-uniform temperature field before death. In this study, a whole body heat transfer model is developed to solve for the steady state temperature field to accurately determine the initial condition before death and quantification of the thermal resistance between the skin and the environment. The Pennes bioheat equation (Pennes, 1948) is implemented to the generated whole body model to determine an appropriate initial temperature distribution in the body. The thermal resistance between the skin and the environment is modeled by an overall heat transfer coefficient. Via adjusting the overall heat transfer coefficient in the model, one can determine a weighted average temperature of the human body to satisfy the energy balance between the human tissue and the blood circulation in the body. From this initial temperature distribution we are able to accurately determine the temperature decay curves presented in later sections.

The whole body model developed in this study is based on a female having a height of 1.68 m and a weight of 68 kg. The body is composed of five main sections: legs, arms, neck, torso, and head, as shown in Fig. 1. The head is modeled as a sphere, the legs, arms, and neck as cylinders, and the torso as a rectangular prism. For each section, a layer of skin, a layer of fat, and a region of muscle are the major components. For the head, there is a thin muscle region, and most of the head is composed of brain tissue with a very high metabolism and a large blood perfusion rate. In the torso, the internal organs are modeled as an embedded rectangular region that also has higher metabolism and blood perfusion rate than that of muscle. Each tissue region is given proper

Table 1
Material properties of different layers.

| Material | Skin | Fat | Muscle | Brain | Internal organs |
|-----------------------------|------|------|--------|-------|-----------------|
| k (W/m K) | 0.47 | 0.21 | 0.642 | 0.49 | 0.592 |
| ρ (kg/m ³) | 1085 | 900 | 1000 | 1080 | 1000 |
| c_p (J/kg) | 3680 | 3500 | 3500 | 3850 | 3500 |

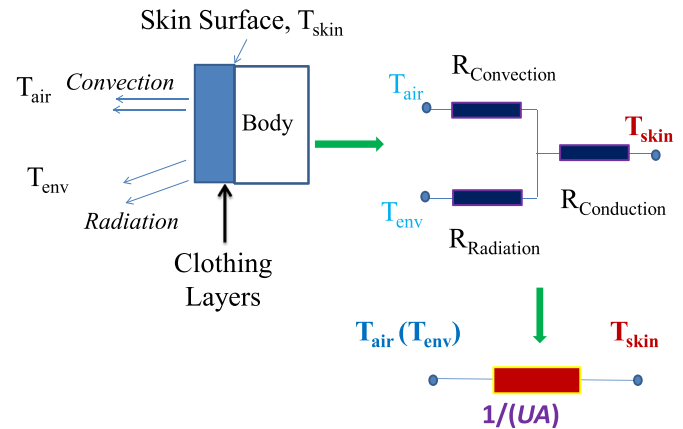


Fig. 2. Schematic diagram of the thermal resistance network between the skin surface of the body and the environment.

physical properties such as the density ρ , thermal conductivity k , and specific heat c_p , listed in Table 1. All properties are obtained from previous studies (Smart and Kaliszán, 2010; Erdmann et al., 2006).

The Pennes bioheat equation (Pennes, 1948) is used as the governing equation determining the steady state temperature field in the modeled human body. It is a modification from the traditional heat conduction equation with an extra source/sink term describing the thermal effect of local blood perfusion. The Pennes bioheat equation is given below:

$$\rho_t c_t \frac{\partial T_t}{\partial t} = \nabla(k_t \nabla T_t) + \omega \rho_a c_a (T_a - T_t) + q_m'' \quad (6)$$

where subscript t denotes tissue, subscript a denotes the arterial blood circulating in the body. At each tissue region, t will be replaced by skin, or fat, or muscle, etc. q_m'' is the volumetric heat generation rate due to metabolism. The thermal effect of the local blood perfusion rate ω is modeled as either a heat sink or source, depending on whether the local tissue temperature T_t is higher or lower than the arterial temperature T_a . In the Pennes bioheat equation, the arterial temperature T_a is considered a constant over the entire body, and may only change with time. Therefore, during a steady state, T_a is a constant such as 37 °C. In tissue region such as the internal organs or the brain, the local tissue temperature is usually higher than 37 °C, therefore, the arterial blood acts as a heat sink there, while in tissue regions such as fingers and toes, it acts as a heat source to warm up those regions. The strength of the blood perfusion term is also proportional to the local blood perfusion rate, the density, and specific heat of blood. The strength of the metabolic heat generation rate is usually considered coupled with the local blood perfusion rate.

How easy to cool a body relies on thermal resistance between the skin surface and the environment (air or water). Layers of clothing a person wears are considered as the conduction resistance. The convection resistance from the outer surface of the clothing to the moving air or water is described by the Newton's law of cooling as $1/(hA)$. Based on the Stefan-Boltzman's law, the equivalent radiation resistance can be $1/(h_r A)$. Combining the three resistances shown in Fig. 2 and assuming that $T_{env} = T_{air}$, one can lump them into a single resistance $1/(UA)$, where U is the overall heat transfer coefficient describing thermal barrier between the skin and the air, and A is surface area of the body. The boundary condition at the skin surface of the body is then formulated as:

$$-k \frac{\partial T_t}{\partial n} \Big|_{surface} = U(T_t - T_{air}) \Big|_{surface} \quad (7)$$

2.2. Determination of the overall heat transfer coefficient, U

Unlike that in previous studies where the thermal resistances due to conduction, convection, and radiation are calculated based on specific environmental conditions, air speed, shape of the body, clothing material and thickness, the thermal resistance in this study is determined based on the achieved thermal equilibrium between the body and its environment (Zhu, 2009). We will utilize the determined temperature field from the Pennes bioheat equation at steady state. The hypothesis here is that the person would have proper clothing, move under the sun or in shade, etc., so that he/she feels thermally comfortable. It implies that the body core temperature should not change when the body establishes a thermal equilibrium with the environment. One thing to achieve equilibrium is the energy balance between blood and tissue in a human body. As mentioned previously, the arterial blood leaves the heart to circulate the body, and exchanges heat with the local tissue. Depending on whether the arterial temperature is higher or lower than the local tissue, the blood loses heat to tissue in regions such as the limbs and muscle, while it gains heat from tissue in regions such as the head and internal organs. When the arterial blood returns back to the heart, its temperature should be the same as that when it leaves the heart, therefore the total energy exchange between the arterial blood and tissue in the body should be zero (Zhu et al., 2009; Zhu, 2010; Paul et al., 2015).

Examining the Pennes bioheat equation, one notes that the blood perfusion term gives the volumetric heat generation rate. Integrating the blood perfusion term over the entire body volume V yields:

$$\iiint_V \omega \rho c_p (T_a - T_t) dV = 0 \text{ at steady state} \quad (8)$$

The integration is zero during steady state when the body establishes thermal equilibrium with its surrounding. Rearranging the above equation yields:

$$\iiint_V \omega \rho c_p T_a dV = \iiint_V \omega \rho c_p T_t dV \text{ at steady state} \quad (9)$$

Since the arterial blood temperature T_a is assumed as a constant of 37 °C, the equation can be further simplified and a weighted average tissue temperature of the whole body, \bar{T}_t , can be expressed as:

$$\bar{T}_t = \frac{\iiint_V \omega T_t dV}{\iiint_V \omega dV} \quad (10)$$

The value of U is adjusted so that a weighted average temperature of the body equals the arterial temperature at 37 °C, when the body establishes a thermal equilibrium with the environment. The arterial temperature T_a is selected as 37 °C, representing normal conditions of a human body. The overall heat transfer coefficient U is initially assumed as 5 W/m² K (Dear et al., 1997) to start the simulation of the steady state temperature field. If the weighted temperature \bar{T}_t is higher than 37 °C, it implies that the previously selected value for U is too small. On the other hand, if \bar{T}_t is lower than 37 °C, the previously selected U value is too large. The overall heat transfer coefficient U is either increased or decreased by an increment of 0.1 W/m² K, one then repeats the above procedures, until the deviation between \bar{T}_t and T_a is less than a threshold of 0.01 °C.

The obtained steady state temperature field is used as the initial condition for the transient temperature simulation of the temperature decay after death. The determined overall heat transfer coefficient to achieve a thermal equilibrium with its surrounding is also used to model the thermal resistance after death, assuming that the person is not added or taken off clothes after

death and the environment is the same as that before he/she is “killed”.

2.3. Postmortem simulation of temperature decay and curve fitting

The human body modeled in the previous section to calculate the overall heat transfer coefficient, U , is also used in this section to determine the temperature decay in the transient process post mortem. The governing heat transfer equation for the “dead” body reduces to the following:

$$\rho_t c_t \frac{\partial T_t}{\partial t} = \nabla \cdot (k_t \nabla T_t) \quad (11)$$

Notice that both the blood perfusion term and the metabolic heat generation rate term vanish in Eq. (11) to simulate post mortem, from the original Pennes bioheat equation. Again, the body consists of regions of skin, fat, muscle, brain, and internal organs. The boundary conditions applied to the transient model are the same as that in the steady state model, shown in the following equation.

$$-k \frac{\partial T_t}{\partial n} \Big|_{\text{surface}} = U(T_t - T_{\text{air}}) \Big|_{\text{surface}} \quad (12)$$

where U is again the overall heat transfer coefficient, the same as that in Section 2.1.

Analytical solutions for typical heat transfer processes suggest that the exponential function behaviors describe the dimensionless or normalized temperature. Therefore, we propose a formula shown below to model the temperature decay at any tissue location, based on our preliminary studies (Bartgis, 2015):

$$\Theta(t) = \frac{T(t) - T_{\text{air}}}{T_{\text{initial}} - T_{\text{air}}} = \begin{cases} 1 & t < t_{\text{delay}} \\ \exp\left[-\frac{t - t_{\text{delay}}}{\tau}\right] & t \geq t_{\text{delay}} \end{cases} \quad (13)$$

where t is the time, $\Theta(t)$ is the normalized temperature at a location, T_{air} is the environmental temperature, T_{initial} is the initial temperature at the same specific location. The temperature is normalized so that Θ only varies between 1, when time is zero, and 0, when time is infinite. Based on our preliminary study, one finds that there is an initial period of t_{delay} , when the temperature at the tissue location is almost unchanged from its initial temperature T_{initial} . After t_{delay} , the temperature decay is proposed to follow an exponential function. As mentioned previously, replacing the temperature decay curve by a proposed formula of temperature drop is for practical use in crime scene investigations, since only one or two measurements are needed to be taken at a specific body location by the detective. The measurements can be used to determine the time of death t based on the temperature measurements, once the coefficients appearing in Eq. (13), such as t_{delay} and τ are known.

The simulated transient temperature decay at either the brain or abdominal location is exported to an Excel file and it is normalized based on the definition of Θ , shown on the left side of Eq. (13). The adjustable parameters here are t_{delay} and τ . Their values are guessed first, although the final fitted values should not be dependent on the initial guesses. The objective function for minimization based on the least square residue fit is defined as:

$$\text{objective function} = \sum_{i=1}^n (\Theta_{\text{actual},i} - \Theta_{\text{curve},i})^2 \quad (14)$$

where n is the number of the total time steps of the simulation of the temperature decays, Θ_{actual} is the normalized temperature decay imported to Excel from the 3-D temperature field simulations, while Θ_{curve} is the normalized temperature values calculated

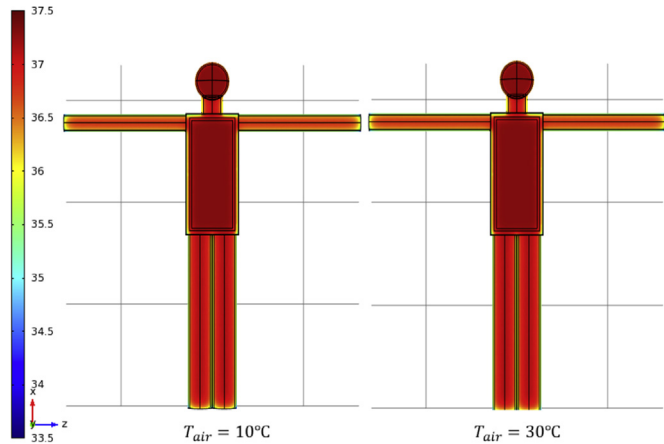


Fig. 3. Cross sectional contours of the initial steady state temperature field for $T_{air}=10\text{ }^{\circ}\text{C}$ and $T_{air}=30\text{ }^{\circ}\text{C}$.

from the proposed temperature decay curve in Eq. (13). Typical optimization processes require that an objective function similar to Eq. (13) is minimized via adjusting the coefficients t_{delay} and τ . In this study, we use the Microsoft Excel 2010 data solver for curve fitting. Excel data solver used the GRG Nonlinear Solving Method for nonlinear optimization. This method works by using the Generalized Reduced Gradient (GRG2) code to find the optimal minimum or maximum value of the objective cell. The decision cells are varied in the code until the objective cell is optimized.

It is expected that all the coefficients in Eq. (13) depend on body size and type, the environmental condition, and measurement locations. In another word, a one-size-fits-all set of the coefficients will not be accurate. In this study, we would like to test the proof of principle of the approach while extracting two sets of the coefficients only at the brain and internal organ locations for a specified environmental condition. The environmental air temperature is then changed to show how the change in air temperature affects the values of the coefficients. All curve fitting results are presented in the next section.

2.4. Numerical simulation using COMSOL

Numerical simulation of the temperature field is carried out by COMSOL 4.2 using finite element methods. Meshing has been generated by COMSOL. A total of 2,326,378 elements are used, and the elements are smaller in the skin and fat layers due to their small thicknesses. The sensitivity of the simulation to element sizes has been tested. When the number of the elements increases by 100%, it results in a less than 1% change in the maximal temperature in the simulated domain.

Table 2

The overall heat transfer coefficient U under different air temperatures and the calculated weighted average body temperature, \bar{T}_t .

| T_{air} ($^{\circ}\text{C}$) | U ($\text{W}/\text{m}^2\text{ }^{\circ}\text{C}$) | \bar{T}_t |
|----------------------------------|-------------------------------------------------------|-------------|
| 10 | 1.2 | 37.00 |
| 12 | 1.25 | 37.01 |
| 15 | 1.5 | 37.00 |
| 18 | 1.75 | 37.00 |
| 20 | 2 | 37.00 |
| 22 | 2.25 | 37.00 |
| 25 | 3 | 36.99 |
| 28 | 4 | 37.00 |
| 30 | 5.5 | 37.00 |

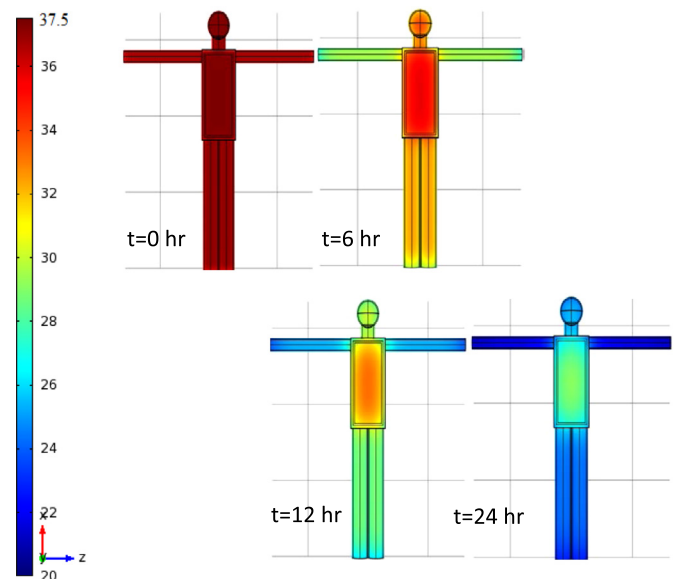


Fig. 4. Temperature contours in the body at various time instants after death.

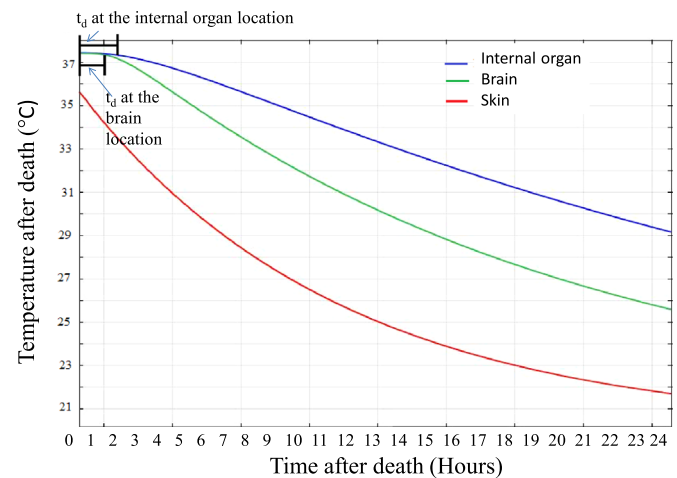


Fig. 5. Typical temperature transients at three body locations: the internal organ, the brain, and the skin surface of the arm.

3. Results

3.1. Steady state temperature field

In this study, the steady state temperature field in the human body is simulated when the body is exposed to one of the nine different air temperatures: 10°C , 12°C , 15°C , 18°C , 20°C , 22°C , 25°C , 28°C , and 30°C . For each air temperature, a value of the overall heat transfer coefficient U is calculated. We make the assumption that the person is thermally comfortable in their environment at the time of death, therefore, the average temperature across the body should be 37°C . Fig. 3 shows the initial temperature fields when the body is exposed to either very cold air (10°C) or very hot air (30°C). The figure provides a cross sectional temperature field for both air temperatures, the hottest temperature in the body is located in the internal organs and the brain, and is approximately 37.3°C , 0.3°C higher than the prescribed arterial blood of 37°C . The temperature is slightly lower in the muscle regions and is the lowest in the skin region. The steady state temperature field agrees very well with previous simulations in the literatures (Huizenda et al., 2001; Moller, 1990; Neilsen et al., 2000; Wang and Zhu, 2007).

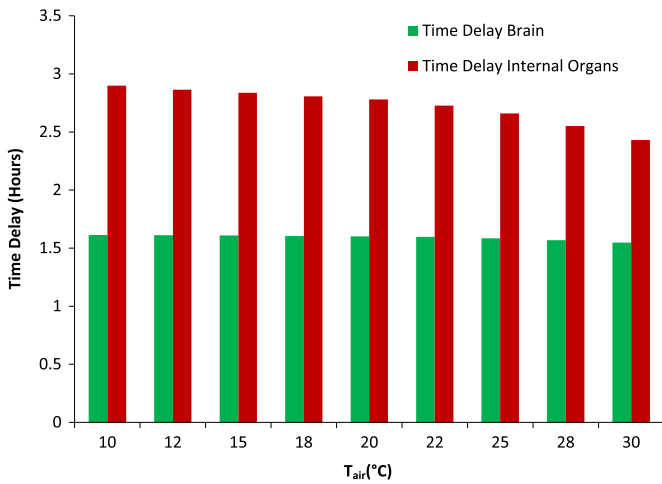


Fig. 6. The initial time delay t_{delay} determined from curve fitting and its dependence on the air temperature and body location.

It is expected that the external air temperature, T_{air} , does not have a significant effect on the temperature field of the body, since the overall heat transfer coefficient U is adjusted to ensure that the person wears appropriate clothing to feel thermally comfortable. The overall heat transfer coefficients are given in Table 2. A smaller U associated with cold air temperature situations implies that the person wearing more clothing. When the air temperature decreases from 30°C to 10°C, the overall heat transfer coefficient decreases almost 80% from 5.5 to 1.2 W/m² °C, suggesting that the thermal resistance increases more than 350%.

3.2. Temperature distribution transients postmortem

Using the initial temperature field obtained in the steady state model, one simulates the temperature field changes after the person is dead. Fig. 4 provides temperature contours of the body in the middle section several hours after the death when the body is exposed to an air temperature of 20 °C. One can see that the extremities cool at the most rapid rate, followed by the head, and the internal organs cool the slowest among all the body regions. After approximately 24 h the only noticeable temperatures above the air temperature are located in the internal organs. This is reasonable since the internal organs have the smallest surface area to volume ratio. Body regions such as the arms have a very high surface area to volume ratio and they start at a temperature lower than 37 °C.

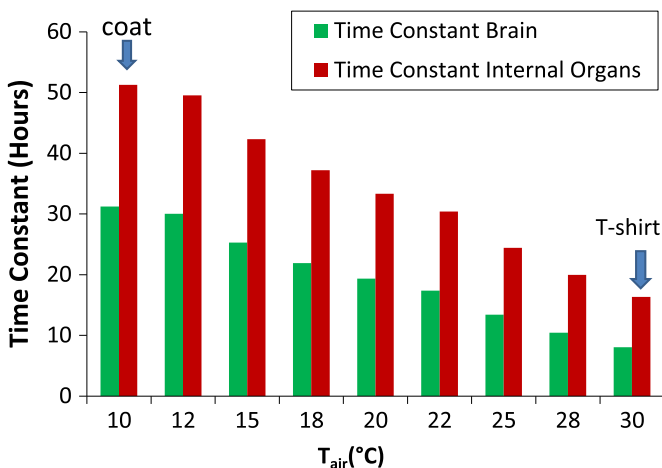


Fig. 7. Effects of the air temperature and body location on the determined time constant.

The arms therefore, establish thermal equilibrium with the environment within 10 h. The deep brain region has a temperature very similar to that in the internal organ before death; however, due to the small size of the head, its temperature decays faster than that of the internal organs.

Three body locations are selected to display their temperature cooling curve after death including the surface of the arm, the center of internal organs, and the center of the brain. The three decay curves for $T_{air}=20$ °C are given in Fig. 5. The temperature decay on the arm skin looks like a typical exponential decay. However, at the center of the internal organs and at the center of the brain, there is a noticeable time delay before the temperature starts to decay exponentially. The initial time delay at the center of the brain is shorter than that at the center of the internal organs. The location at the skin surface of the arm is not suitable for determining the time of death since its initial temperature before death can be significantly affected by various factors, while both the internal organs and brain almost always starts with a certain 37.3 °C, 0.3 °C higher than the arterial blood temperature. Even after 24 h, the temperature at the internal organs is still 9 °C above the environmental temperature, while the temperature in deep brain is approximately 5 °C above T_{air} . The simulation results demonstrate that the internal organ is a better location than the brain for determining time of death, especially when more than 24 h have passed after the death.

The R^2 values of all the curve fittings are larger than 0.998 when Eq. (13) is used to fit the simulation curves, implying excellent curve fitting. The fitted curve for the temperature decay at the brain location when the body exposed to 20 °C air after death is expressed as:

$$\theta(t) = \frac{T(t) - T_{air}}{T_{initial} - T_{air}} = \begin{cases} 1 & t < 5763 \\ \exp\left[-\frac{t - 5763}{69637}\right] & t \geq 5763 \end{cases} \quad (15)$$

This formula can be very useful for the detective to determine the time of death with a single temperature measurement at the internal organ location. For example, if the measured temperature is 32 °C, and $T_{air}=20$ °C, based on the formula, the time when the measurement is taken can be easily solved as 31,075 s or 8.6 h.

The effect of the air temperature on the cooling curve is illustrated in Figs. 6 and 7, when the temperature measurement is taken at either the brain location or the internal organ location. At the head center, the fitted t_{delay} varies slightly around 1.6 h for all the air temperatures, while t_{delay} is longer at the center of the internal organs, varying from 2.4 to 2.9 h. There are almost 1.6–2.9 h when the temperature does not change significantly from the initial 37.3 °C at the measurement site. Therefore, it would not be very accurate to determine the time of death within this initial window. Fig. 7 gives the time constant of the exponential function for the brain location, varying from 28,930 s (~8 h) for $T_{air}=30$ °C to 112,465 s (~31 h) for $T_{air}=10$ °C. The time constant provides the measurement window after death to be between 8 h to 31 h, depending on the air temperature. Similarly, the trends at the internal organ location are very similar to that at the brain location. It would have taken much longer time to cool down the torso than the brain. When the air temperature is 10 °C, the time constant for the internal organ location is 64% longer than that for the brain location, while the time constant at the internal organ site doubles that at the brain site when the air temperature is 30 °C. The results in Fig. 7 suggest that the measurement window after death at the internal organ location is approximately between 16 h and 51 h, depending on the air temperature. The time constant is longer when the body is exposed to colder air. Note that a person usually wears more clothing when it is colder outside to keep the body warm and comfortable. Assuming that after death, the body

has the same clothing as that before the death, the larger thermal resistance due to clothing in colder air would slow down heat conduction from the body core to the skin, leading to a slower cooling rate of the body.

4. Discussion

The presumed time of death in criminal justice is often used to implicate or exonerate a person of interest. The typical practice substitutes a temperature measured at a body site at the scene into a simple formula to roughly estimate the time of death. The developed whole body heat transfer model in this study is the first attempt to address some, however, not all of the limitations of the formulae currently used in practices, namely, the inaccuracy of the estimation of the overall heat transfer coefficient and lack of description of thermal effects of body shape and/or size on the postmortem prediction. It still has many limitations that should be addressed in the future to make the prediction of time of death within an acceptable range.

This research only generates one body model based on a female body with European decent. It is well known that the size and shape of the body should have profound influence on the initial temperature field of the body, and the cooling process after death. Therefore, it is unlikely that the generated cooling curves in the study can be readily applied to other body shapes and sizes. Therefore, similar efforts have to be continued to develop more body models based on a variety of the shapes and sizes. In addition, there are significant tissue structural differences between a female body and a male body. Women tend to sweat less and have a thicker fat layer while men typically have a higher metabolic heat rate (Spieker et al., 1999). Women also carry more of their weight in their hips and chest where men tend to carry more of their weight in their gut. The placement of extra fat or muscle could lead to differences in the temperature decay curve. A body with the internal organ volume but a fat layer twice the thickness will have more insulation, in theory slowing heat transfer from the internal organs. The same may happen with a body with a muscle layer twice the size of the model used in this study. Height, fitness, ethnicity, and gender, all play significant roles in the shape of the body. Studies have shown that Asians typically have a lower body mass index than Europeans (Wang et al., 1994). It is very important to also take those factors into considerations when one models other types of bodies.

With advancement in computational resources, the whole body model can be further improved via including more structures within the geometry. For example, the bones inside a body have different thermal properties from that of muscle or fat. Due to their significant portion in a human body, future studies may be needed to evaluate whether including them would have significantly changed the cooling time of those cooling curves. The internal organs in this study are also modeled as one large clump. It would have been more accurate to model internal organs individually since their blood perfusion rates and metabolic rates are quite different from each other. Future studies are needed to understand whether separation of the internal organs would affect the results and help pinpoint which internal organ location is the best for temperature measurement and determination of time of death.

In the current model, one assumes that the person is wearing appropriate clothing for the environment they are in, and the environmental air temperature is kept the same postmortem. In reality, the body could have been moved from inside to outside, the external air temperature may change after death, and the person's clothes could be removed/added. In future studies the model could be modified to account for the non-uniform air

temperature variation for the simulation duration, brief raining or snow conditions after death implying change of environment so that the overall heat transfer coefficient should be re-calculated for the transient temperature decay simulations. Other details can be added to the model, including whether the person is lying on the floor, grass, sitting on the chair, therefore, leading to more realistic and more accurate predictions of the cooling processes of a body.

In summary, we have articulated the limitations of current practices of determining postmortem interval in practice, and elaborated the rationales of simulating temperature cooling curves based on development of a rigorous 3-D whole body heat transfer model. The results given in this study has demonstrated the accuracy of determining the overall heat transfer coefficient or the thermal resistance between the skin and air via an indirect approach assuming thermal equilibrium. The curve fitting techniques used in this study have been tested to understand how air temperature affects the overall heat transfer coefficient, the initial time delay, and the time constant associated with the body cooling.

References

- Bartgis, C., 2015. Development of a Three Dimensional Whole Body Heat Transfer Model to Determine the Post Mortem Interval. University of Maryland Baltimore County, Maryland, USA.
- Bergman, T., Lavine, A., Incopera, F., Dewitt, D., 2011. Fundamentals of Heat and Mass Transfer. John Wiley and Sons, Hoboken, NJ.
- Crowther, M.A., White, B., 1988. On Soul and Consequence. The Medical Expert and Crime: 150 Years of Forensic Medicine in Glasgow. Aberdeen University Press, Aberdeen.
- Dear, R., Arens, E., Hui, Z., Oguro, M., 1997. Convective and radiative heat transfer coefficients for individual human body segments. *Int. J. Biometeorol.* 40, 141–156.
- Erdmann, B., Lang, J., Seebass, M., 2006. Optimization of temperature distributions for regional hyperthermia based on a nonlinear heat transfer model. *Ann. N. Y. Acad. Sci.* 858, 36–46.
- Guharaj, P., 1982. Forensic Medicine Bombay. Orient Longman Ltd., India.
- Huizenda, C., Hui, Z., Arens, E., 2001. A model of human physiology and comfort for assessing complex thermal environments. *Build. Environ.* 36, 691–699.
- Mall, G., Eisenmenger, W., 2004a. Estimation of time since death by heat-flow finite-element model. Part 1: method, model, calibration and validation. *Leg. Med.* 7, 1–14.
- Mall, G., Eisenmenger, W., 2004b. Estimation of time since death by heat-flow finite-element model. Part II: application to non-standard cooling conditions and preliminary results in practical casework. *Leg. Med.* 7, 69–80.
- Moller, D., 1990. Advanced Simulation in Biomedicine. Springer Science Business Media, LLC, New York, NY.
- Neilsen, B., Hyldig, T., Bidstrup, F., Gonzalez-Alonso, J., Christoffersen, G.R.J., 2000. Brain activity and fatigue during prolonged exercise in the heat. *Eur. J. Physiol.* 442, 41–48.
- Pennes, W., 1948. Analysis of tissue and arterial blood temperature in the resting human forearm. *J. Appl. Physiol.* 1, 93–122.
- Payne-James, J., Jones, R., Karch, S., Manlove, J., 2011. Simpson's Forensic Medicine. Hodder and Stoughton Ltd., London, England.
- Paul, A.K., Zachariah, S., Zhu, L., Banerjee, R.K., 2015. Predicting core body temperature during cold water immersion and exercise: application of a tissue-blood interactive whole body model. *Heat Transf.* 68 (6), 598–618.
- Smart, J., Kaliszan, M., 2010. Prediction of time of death using a heat transport model. In: Proceedings of the COMSOL Conference, Boston.
- Spieker, M., Hayes, L., Wissler, E., Colvin, D., 1999. Analysis of gender based thermal regulation. *Adv. Heat Mass Transf. Biotechnol.* 44, 25–29.
- Wang, J., Thornton, J., Russell, M., Burastero, S., Heymsfield, S., 1994. Asians have lower body mass index (BMI) but higher percent body fat than do whites: comparisons of anthropometric measurements. *Am. J. Clin. Nutr.* 60, 23–28.
- Wang, J., Zhu, L., 2007. Targeted brain hypothermia induced by an interstitial cooling device in human neck: theoretical analysis. *Eur. J. Appl. Physiol.* 101, 31–40.
- Zhu, L., 2009. Heat transfer in applications in biological systems. In: *Biomedical Engineering & Design Handbook*, Chapter 2, Volume 1: Bioengineering Fundamentals, McGraw-Hill, pp. 2.33–2.67.
- Zhu, L., 2010. Recent developments in biotransport. *ASME J. Thermodyn. Sci. Appl.* 2 (1), 1–11.
- Zhu, L., Schappeler, T., Cordero-Tumangday, C., Rosengart, A.J., 2009. Thermal interactions between blood and tissue: development of a theoretical approach in predicting body temperature during blood cooling/rewarming. *Adv. Numer. Heat Transf.* 3, 197–219.